Cd36 knockout mice are protected against lithogenic diet-induced gallstones

Yan Xie,* Vincenza Cifarelli,† Terri Pietka,† Elizabeth P. Newberry,* Susan M. Kennedy,* Amin Khalifeh-Soltani,§ Robin Clugston, Kamran Atabai,§ Nada A. Abumrad,[1,2,†] and Nicholas O. Davidson[1,2,*]**

Gastroenterology Division,* Center for Human Nutrition,† Department of Medicine, Washington University School of Medicine, St. Louis, MO; Cardiovascular Research Institute,§ Department of Medicine, University of California, San Francisco, CA; and Department of Physiology,** University of Alberta, Edmonton, Canada

ORCID ID: 0000-0003-2375-8116 (N.O.D.)

Abstract The scavenger receptor and multiligand transporter CD36 functions to promote cellular free fatty acid uptake and regulates aspects of both hepatic and intestinal cholesterol metabolism. However, the role of CD36 in regulating canalicular and biliary cholesterol transport and secretion is unknown. Here, we show that germline *Cd36* knockout (KO) mice are protected against lithogenic diet (LD)-induced gallstones compared with congenic (C57BL6/J) controls. *Cd36* KO mice crossed into congenic *L-Fabp* KO mice (DKO mice) demonstrated protection against LD-induced gallstones, reversing the susceptibility phenotype observed in *L-Fabp* KO mice. DKO mice demonstrated reduced biliary cholesterol secretion and a shift into more hydrophophilic bile acid species, without changes in either BA pool size or fecal excretion. In addition, we found that the mean and maximum force of gallbladder contraction was increased in germline *Cd36* KO mice, and gallbladder lipid content was reduced compared with wild-type controls. Finally, whereas germline *Cd36* KO mice were protected against LD-induced gallstones, neither liver- nor intestine-specific *Cd36* KO mice were protected. Taken together, our findings show that CD36 plays an important role in modifying gallstone susceptibility in mice, at least in part by altering biliary lipid composition, but also by promoting gallbladder contractility.—Xie, Y., V. Cifarelli, T. Pietka, E. P. Newberry, S. Kennedy, A. Khalifeh-Soltani, R. Clugston, K. Atabai, N. A. Abumrad, and N. O. Davidson. ***Cd36* knockout mice are protected against lithogenic diet-induced gallstones. *J. Lipid Res*. 2017.** 58: **1692–1701.**

Supplementary key words canalicular cholesterol • bile acid • phospholipid • liver fatty acid binding protein • gallbladder motility

Gallstone disease and its comorbidities continue to represent a healthcare and economic challenge in the developed world (1). Our understanding of the pathogenesis of cholesterol gallstone disease includes both genetic and environmental risk factors, events that converge on pathways that regulate hepatic cholesterol metabolism and canalicular lipid secretion (2, 3). Genome-wide association studies implicate susceptibility loci with functions in cholesterol metabolism and transport, in particular the canalicular cholesterol transporter ABCG5/G8 (4, 5). Other studies, using inbred mouse strains, have led to the identification of quantitative trait loci and corresponding positional candidate genes that predispose to lithogenic diet (LD)-induced gallstones (6, 7).

Studies examining environmental and genetic risk factors suggest that several distinct metabolic pathways modify gallstone susceptibility. These pathways include those regulated by nuclear hormone receptors involved in sterol and bile acid sensing (8, 9), as well as pathways more broadly involved in hepatic lipid utilization and metabolic channeling. For example, mice with germline deletion of *L-Fabp*, while protected against diet-induced hepatic steatosis (10, 11) demonstrated increased LD-induced gallstone formation, at least in part through augmented canalicular cholesterol secretion (12). Similarly, germline deletion of *Elovl6* attenuated hepatic steatosis in *Ldlr* KO mice, yet enhanced gallstone susceptibility (13). Here, we asked whether the multiligand class B scavenger receptor CD36 might play a role in modifying hepatic cholesterol utilization and export. This possibility was in part predicated on findings that mouse hepatic CD36 expression is increased in response to

N.O.D. was supported by National Institutes of Health Grants HL-38180, DK-112378, DK-56260, DK52574, and Murine and Advanced Imaging Cores. N.A.A. was supported by National Institutes of Health Grants DK060022 and DK033301 and by Adipocyte Biology and Molecular Nutrition Core of the Nutrition Obesity Research Center Grant P30 DK056341. K.A. was supported by National Institutes of Health Grant R01DK110098 and American Heart Association Grant 15GRNT25080286. A.K-S. was supported by an American Heart Association fellowship and American Brain Foundation Fellowship 14POST18580033. The content is solely the responsibility of the authors and does not necessarily represent the official views of the National Institutes of Health.

Manuscript received 2 May 2017 and in revised form 19 June 2017.

Published, JLR Papers in Press, June 20, 2017
DOI https://doi.org/10.1194/jlr.M077479

Abbreviations: bw, body weight; CCK, cholecystokinin; *Cd36-IKO*, intestine-specific *Cd36* KO; *Cd36-LKO*, liver-specific *Cd36* KO; ChMC, cholesterol monohydrate crystal; DKO, *Cd36*, *L-Fabp* double KO; LD, lithogenic diet.

[1] N. A. Abumrad and N. O. Davidson laboratories contributed equally to this work.

[2] To whom correspondence should be addressed.

e-mail: nod@wustl.edu (N.O.D.); nabumrad@wustl.edu (N.A.A.)

high-fat diet-induced obesity and other findings that adenoviral-mediated hepatic CD36 overexpression increased hepatic FFA uptake and steatosis (14). In addition, CD36 has been shown to regulate cholesterol uptake, utilization, and secretion from both the small intestine (15, 16) and mouse peritoneal macrophages (17).

Beyond the metabolic alterations alluded to above, there is a role for altered gallbladder motility in promoting gallstone susceptibility, evidenced by findings in both *Cck* KO mice and in *Cckr1* KO mice (18, 19). These findings, coupled with findings that CD36-dependent signaling promotes secretin and cholecystokinin (CCK) release from enteroendocrine cells (20), raised the question of whether CD36 might function more broadly in modifying gallstone susceptibility, specifically via alterations in gallbladder contractility. Here, we show that germline *Cd36* KO mice are protected against LD-induced gallstones via mechanisms including alterations in biliary cholesterol secretion, bile acid composition, and enhanced gallbladder contractility.

MATERIALS AND METHODS

Animals and diets

All animals were maintained in a C57BL6/J background and housed on a 12 h light-dark cycle, in a full-barrier facility. Ten- to 12-week-old male mice were fed either standard rodent chow (PicoLab Rodent Diet 20, fat 4.5%, cholesterol 0.015%) or an LD (Research Diet no. 960393, fat 18.8%, cholesterol 1.2%, and cholic acid 0.5%) for 2–4 weeks, as indicated. *L-Fabp*$^{-/-}$ mice (12) and *Cd36*$^{-/-}$ mice (21) were used in crosses to generate a line of compound *Cd36*, *L-Fabp* double KO mice (hereafter referred to as DKO). *Cd36* conditional KO mice were generated from *Cd36*$^{flox/flox}$ mice (22) crossed into either Albumin-Cre or Villin-Cre lines (Jax) to generate the compound line of tissue-specific KO (either liver- or intestine-specific) mice. Age-matched and cohoused littermates were used as controls. All animal protocols were approved by the Washington University Animal Studies Committee and followed guidelines outlined by the National Institutes of Health.

Tissue and serum lipid determinations

Animals were euthanized after a 4 h fast. Liver and serum were collected and frozen at −80°C until analyzed. Serum triglyceride and cholesterol were measured by using reagents from Wako (Neuss, Germany), an L-Type Triglyceride M Kit (catalog nos. 465-09791 and 461-09891), and the cholesterol E kit (catalog no. 439-17501). Hepatic or, where indicated, gallbladder lipids were extracted by using chloroform: methanol (2:1) and triglyceride, cholesterol, free cholesterol, free fatty acids, and phospholipids enzymatically with the indicated Wako reagent kits: the L-Type Triglyceride M Kit, the cholesterol E kit, the free cholesterol E kit (catalog no. 435-35801), the HR series NRFA-HR2 kit (catalog nos. 991-34891 and 995-34791), and the phospholipid C kit (catalog no. 433-36201).

Gallstone analysis and gallbladder bile cholesterol saturation index

Animals were fed a LD for 4 weeks as indicated in the relevant figure legends and euthanized after a 4 h fast. Fresh gallbladder bile was immediately analyzed by polarizing microscopy using a visual scale with the following criteria: 0, absence of cholesterol monohydrate crystals (ChMCs), 1, small number of ChMCs (<3 per high power field); 2, many ChMCs (≥3 per high power field); 3 = aggregated ChMCs; and 4 = presence of "sandy" light-translucent stones or "solid" light-opaque stones (7). Gallbladder bile cholesterol content was measured enzymatically after chloroform: methanol (2:1) extraction. Gallbladder bile phospholipids and bile acid content were analyzed enzymatically by using the total bile acids assay kit (BQ 092A-EALD, BQ Kits, San Diego, CA). Cholesterol saturation indices in gallbladder bile were calculated by using published parameters (23).

Biliary lipid secretion and bile acid pool size

Mice were fed a LD for 2 weeks and anesthetized after a 4 h fast. An external bile fistula was established surgically, and bile samples collected during the first 15 min were discarded. Bile samples were collected for another 60 min and used for biliary lipid secretion analysis. Hepatic bile volume was determined gravimetrically assuming a density of 1 g·ml^{-1}. Biliary phospholipids, cholesterol, and total bile acid content were determined enzymatically. Biliary lipid secretion values are presented as nmol/min/kg body weight (bw). Individual bile acid species were determined by using HPLC as previously described (12) and with commercially obtained standards. The hydrophobicity index was calculated by using published parameters (24). Bile acid pool size and fecal bile acids excretion were determined in groups of mice fed a LD for 2 weeks. For bile acid pool size, the liver, gallbladder, and intestine were homogenized together, and bile acid content was measured as previously detailed (12). For fecal bile acid excretion, feces from individual animals were collected for up to 72 h. Feces were homogenized, and bile acid content was determined enzymatically.

Gene expression analysis

Hepatic total RNA or proximal intestinal RNA was extracted and cDNA was prepared by using an ABI high-capacity cDNA reverse transcription kit with 1 μg of total RNA. Real-time quantitative PCR used cDNAs from four to six animals per group and was performed in triplicate on an ABI Prism7000 sequence detection system using SYBR Green PCR Master Mix (Applied Biosystems) and primer pairs (provided on request) designed by Primer Express software (Applied Biosystems). Relative mRNA abundance is expressed as fold change to WT control after normalization to own GAPDH. To detect hepatic CD36 and L-Fabp protein, 50 mg of liver was homogenized in 0.5 ml of buffer containing 25 mM HEPES, 150 mM NaCL, 0.5 mM EDTA, 0.1% SDS, 1% Triton, and protease inhibitors, by using the Bullet Blender^{R} system (Next Advance) with 1 mm zirconium oxide beads. Aliquots of 50 μg of protein were separated by 4–20% SDS-PAGE gel. Samples of terminal ileum protein were used to prepare total and membrane extracts as described (12, 25) by using the Bullet Blender^{R} system with 1 mm steel beads. In brief, approximately 50–100 mg of full-thickness ileum was homogenized in 0.8 ml of lysis buffer (250 mM sucrose and 10 mM Triethanolamine-HCL, pH 7.6) containing protease inhibitors (Complete protease inhibitor mixture, Roche Diagnostics). The crude preparation was centrifuged at 2,500 *g* for 10 min, and the supernatant was recentrifuged at 30,000 *g* for 60 min at 4°C by using a Beckman MLA-130 rotor. The resulting membrane pellet was resuspended in solubilization buffer [15% SDS, 8 M Urea, 10% (w/v) sucrose, 62.5 mM Tris-HCL, and 5 mM dithiothreitol, pH 6.8]. Membrane proteins (50 μg) were separated on 10% SDS-PAGE gel, transferred to Immobilon®-P membranes (Millipore, Billerica, MA), and immunoblotted with 1:2,000 goat anti-mouse CD36 (16), 1:2,000 rabbit anti-mouse L-Fabp (26), 1:300 rabbit anti-mouse Fgf15, and 1:1,000 monoclonal rabbit anti-mouse Asbt antibody (generous gifts from Dr. Paul A Dawson), and quantitated by Kodak Image software.

Gallbladder contractility studies. Gallbladders were taken from age- and sex-matched (male) chow-fed WT and *Cd36*$^{-/-}$

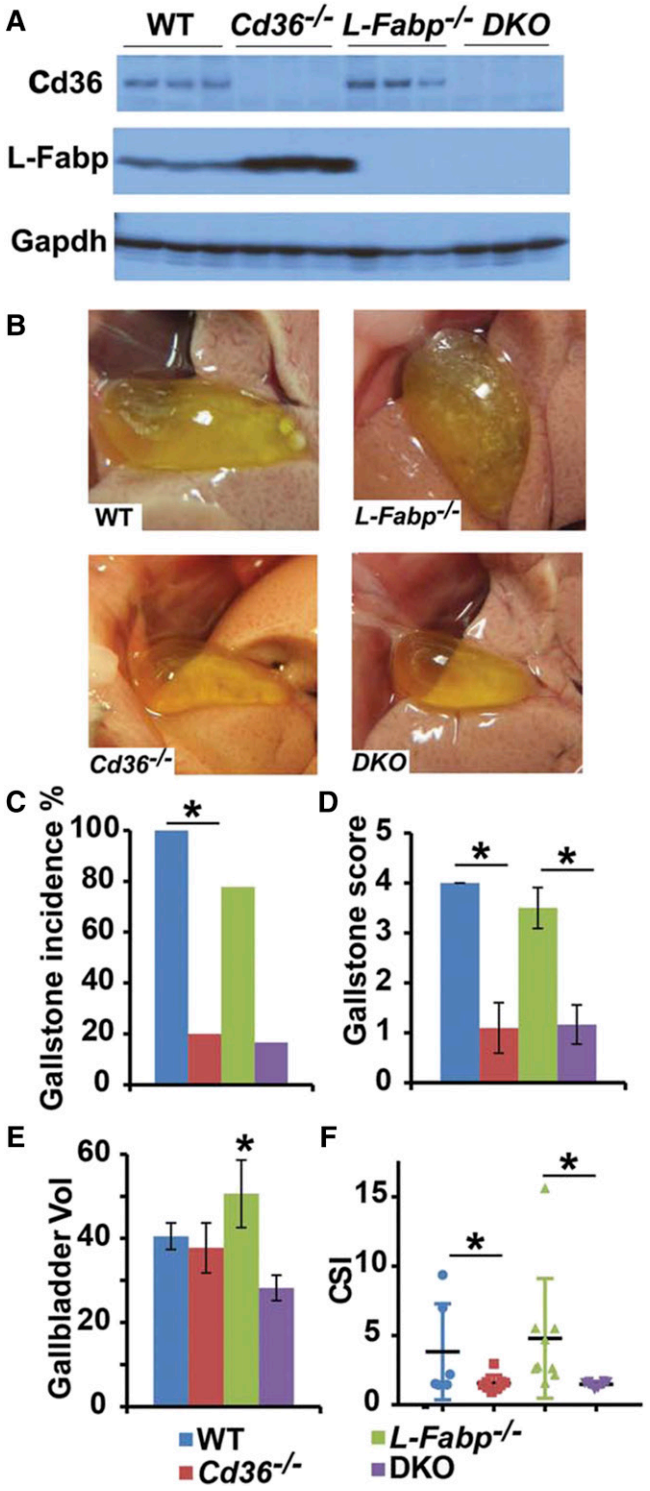

Fig. 1. Cd36$^{-/-}$ mice are protected against gallstones, and Cd36 deletion confers protection in L-Fabp$^{-/-}$ mice (DKO mice) after 4 weeks of LD feeding. A: Hepatic CD36 and L-Fabp protein expression were determined by Western blotting of total liver extracts. CD36 protein was not detected in either Cd36$^{-/-}$ mice or DKO liver, and L-Fabp protein was likewise not detected in either L-Fabp$^{-/-}$ or DKO liver as predicted. B: Representative gross appearances of gallbladder after 4 weeks of LD feeding. Gallbladders from WT and L-Fabp$^{-/-}$ mice appear opaque with visible solid stones, whereas gallbladders from Cd36$^{-/-}$ mice and DKO are transparent without visible stones. Gallstone incidence (C) and gallstone score (D) were significantly reduced in both Cd36$^{-/-}$ mice and in DKO mice. E: Gallbladder volume was determined gravimetrically (Materials and Methods). F: Cholesterol saturation index (CSI) of gallbladder bile was calculated as described in Materials and Methods. Cd36$^{-/-}$ and DKO mice demonstrate a similar decrease in CSI compared with WT and L-Fabp$^{-/-}$ mice, n = 6–12 mice per group. The data associated with different superscript letters are significantly different ($P < 0.05$). The data reflect the mean ± SE. *Statistically significant differences ($P < 0.05$).

mice. Both surfaces of the excised gallbladder were gently cut and washed with PBS and attached to a force transducer (Radnoti 8-chamber tissue-organ bath system) exactly as described (27). Gallbladders were immersed in warmed, oxygenated buffer for 30 min before the addition of the indicated concentrations of methacholine and KCl. Resting tension of 0.5 g was applied after each treatment as previously described (28).

Statistical analysis

Statistical significance was determined with one-way ANOVA for multiple group comparisons and *t*-testing as a post hoc test for comparing different pairs using GraphPad Prism 7 software (GraphPad, San Diego, CA). Data are expressed as the mean ± SE unless otherwise noted.

RESULTS

Cd36 deletion protects against LD-induced gallstones and attenuates gallstone susceptibility in *L-Fabp* KO mice

Our first objective was to ascertain a role for CD36 in LD-induced gallstone susceptibility. Mice of the indicated genotype (**Fig. 1A**) were studied after consuming a LD for 4 weeks, with the data showing that *Cd36*$^{-/-}$ mice (Fig. 1A) exhibited a striking reduction in gallstone incidence with correspondingly reduced gallstone score and reduced cholesterol saturation index (Fig. 1B). Furthermore, when crossed into germline *L-Fabp*$^{-/-}$ mice, both *Cd36*$^{-/-}$and the compound DKO mice (Fig. 1A, B) were protected, as evidenced by the visually clear appearance of the gallbladder, decreased cholesterol saturation index, and reduced gallbladder volume (Fig. 1B). We observed increased abundance of L-Fabp protein in livers from LD-fed *Cd36* KO mice compared with WT controls (Fig. 1A), an observation whose underlying mechanisms remain to be elucidated. However, these findings point to a role of CD36 as a modifier of murine gallstone susceptibility in mice either WT or null for the *L-Fabp* allele.

Gallstone protection in *Cd36*$^{-/-}$ mice is associated with alterations in biliary lipid secretion

Hepatic lipid content across the genotypes in LD-fed mice indicated no major differences in total or free cholesterol content, but revealed increased bile acid content in both *Cd36*$^{-/-}$ and DKO mice (**Table 1**). We next examined the concentration and relative distribution of the most abundant individual bile acid species from newly secreted bile samples in each genotype. These data revealed increased biliary concentration of taurobetamuricholic acid in LD-fed *Cd36*$^{-/-}$ mice (**Fig. 2A**) with a shift in relative

TABLE 1. Hepatic lipid content in LD-fed mice of the indicated genotype

Genotype	TC	FC	CE	PL	FFA	BA
WT (6)	159.8 ± 22.9	27.5 ± 1.3	132.3 ± 22.9	85.6 ± 2.4	86.6 ± 5.6[a]	21.8 ± 9.1[a]
Cd36$^{-/-}$ (6)	159.8 ± 10.4	31.0 ± 4.8	128.8 ± 10.9	92.5 ± 5.0	85.0 ± 4.9[a]	27.1 ± 15.1[a]
L-Fabp$^{-/-}$ (5)	147.5 ± 11.6	24.0 ± 3.7	123.6 ± 12.3	95.8 ± 4.6	80.7 ± 9.1[a]	19.6 ± 4.1[a]
DKO (6)	159.4 ± 24.9	32.4 ± 1.9	127.0 ± 26.7	93.9 ± 2.7	132.9 ± 10.9[b]	33.2 ± 11.2[a]

Mice from four experimental groups (n per group) were fed a LD for 4 weeks. Hepatic lipids were extracted and analyzed (Materials and Methods). Hepatic lipid content is expressed as mean ± SE (μg/mg protein), except FFA (nmol/mg protein). The difference between values associated with different superscript letters for the parameters indicated in each vertical column is statistically significant ($P < 0.05$). BA, bile acid; CE, cholesteryl ester; FC, free cholesterol; FFA, free fatty acid; PL, phospholipid; TC, total cholesterol.

taurobetamuricholic acid distribution favoring enrichment in both *Cd36*$^{-/-}$ and DKO mice (Fig. 2B). The net impact of these relatively subtle, albeit significant, differences in bile acid species includes a significant decrease in hydrophobicity index (24) in both *Cd36*$^{-/-}$ and DKO mice (Fig. 2C). Daily fecal bile acid excretion (Fig. 2D) and total bile acid pool sizes (Fig. 2E) were comparable across the genotypes, suggesting that there were no major shifts in enterohepatic cycling.

We further examined biliary lipid secretion rates in the various genotypes, using a shorter (2 week) LD feeding interval. This interval was selected to circumvent the inevitable bile duct obstruction that accompanied the extensive gallstone formation in both WT and *L-Fabp*$^{-/-}$ mice noted above. Those findings revealed increased biliary cholesterol secretion in *L-Fabp*$^{-/-}$ mice compared with both WT and *Cd36*$^{-/-}$ mice (**Table 2**). There was a trend to decreased biliary cholesterol secretion in *Cd36*$^{-/-}$ mice (175 nmol/min/kg bw) compared with WT controls (210 nmol/min/kg bw) and in DKO mice (222 nmol/min/kg bw) compared with *L-Fabp*$^{-/-}$ mice (298 nmol/min/kg bw), without changes in bile flow rate by genotype (Table 2). Taken together, these findings suggest that altered biliary bile acid composition and attenuated cholesterol secretion in LD-fed *Cd36*$^{-/-}$ mice may in combination contribute to the protection observed against gallstone formation.

Gallstone protection in *Cd36*$^{-/-}$ mice is associated with alterations in genes regulating hepatic and intestinal cholesterol and bile acid metabolism

We next sought to understand the mechanisms underlying the alterations in biliary lipid secretion noted above by profiling the expression of several mRNAs involved in hepatic cholesterol and bile acid homeostasis. We observed decreased expression of hepatic Cyp7a1 in *L-Fabp*$^{-/-}$ mice as previously demonstrated (12) and also in both genotypes of *Cd36*$^{-/-}$ mice, which was accompanied by increased Cyp8b1 expression in LD-fed *Cd36*$^{-/-}$ and DKO mice (**Fig. 3A**). The increased expression of hepatic Cyp8b1 mRNA in *Cd36*$^{-/-}$ and DKO mice was not accompanied by increased biliary taurocholate concentration, as might be predicted (29, 30), but it bears emphasis that those bile acid distribution data (Fig. 2A and above) reflect mice fed supplemental cholic acid as part of the LD regimen. We also observed decreased expression of HMGR mRNA in *Cd36*$^{-/-}$ and DKO mice, findings suggesting that de novo hepatic cholesterol production may be decreased, a possibility consistent with the decreased secretion of biliary cholesterol noted above, as well as earlier findings suggesting decreased de novo lipogenesis in *Cd36*$^{-/-}$ mice (31).

We next turned to an examination of a panel of intestinal genes involved in cholesterol and bile acid metabolism, in part guided by previous findings of regionally specific adaptive alterations in their expression in germline *Cd36*$^{-/-}$ mice (16). Our findings revealed decreased expression of NPC1L1 mRNA and protein in both *Cd36*$^{-/-}$ and DKO mice (Fig. 3B, C) and increased expression of SRB1 in proximal intestinal samples (Fig. 3B, C) along with decreased mRNA abundance of ABCG5/G8 in germline *Cd36*$^{-/-}$ mice (Fig. 3B). These findings point to the possibility of altered intestinal cholesterol uptake and absorption in LD-fed *Cd36*$^{-/-}$ and DKO mice, consistent with prior findings showing decreased cholesterol absorption in chow-fed *Cd36*$^{-/-}$ mice (15, 16). We observed increased ileal expression of FGF15 expression in *L-Fabp*$^{-/-}$ mice, but no change in ASBT expression in any genotype. Taken together, these findings suggest a range of adaptive changes in enterohepatic cholesterol and bile acid metabolism in LD-fed mice of the respective genotypes, raising the possibility that either intestinal- or hepatic-specific *Cd36* deletion might reveal a dominant pathway that confers protection against gallstones.

Neither intestine- nor liver-specific Cd36 deletion protects against LD-induced gallstone formation

We first examined intestine-specific *Cd36* KO mice (*Cd36-IKO*), which were generated as previously documented (22) and fed a LD for 4 weeks. We found that both flox/flox (i.e., CD36 WT) controls and *Cd36-IKO* mice demonstrated gallstones, with no differences noted in any of the physical parameters of score or gallbladder volume (**Fig. 4A–**D). In addition, there were no differences by genotype in hepatic lipid or bile acid content (Fig. 4E).

Using a similar approach, we generated liver-specific *Cd36* KO mice (*Cd36-LKO*) using Albumin-Cre mice (Jax). We documented liver-specific recombination at the *Cd36* locus (**Fig. 5A**) and knockdown of hepatocyte CD36 (Fig. 5B), demonstrating that this strategy induced a decrease in CD36 expression in hepatocytes at baseline in chow-fed mice. Unexpectedly, we observed that total hepatic CD36 abundance appeared slightly increased in LD-fed *Cd36-LKO* compared with WT controls (Fig. 5C), suggesting that hepatocyte CD36 is likely only a minor component of overall hepatic CD36 expression. Both WT and *Cd36 LKO* mice demonstrated gallstones with no difference by genotype in

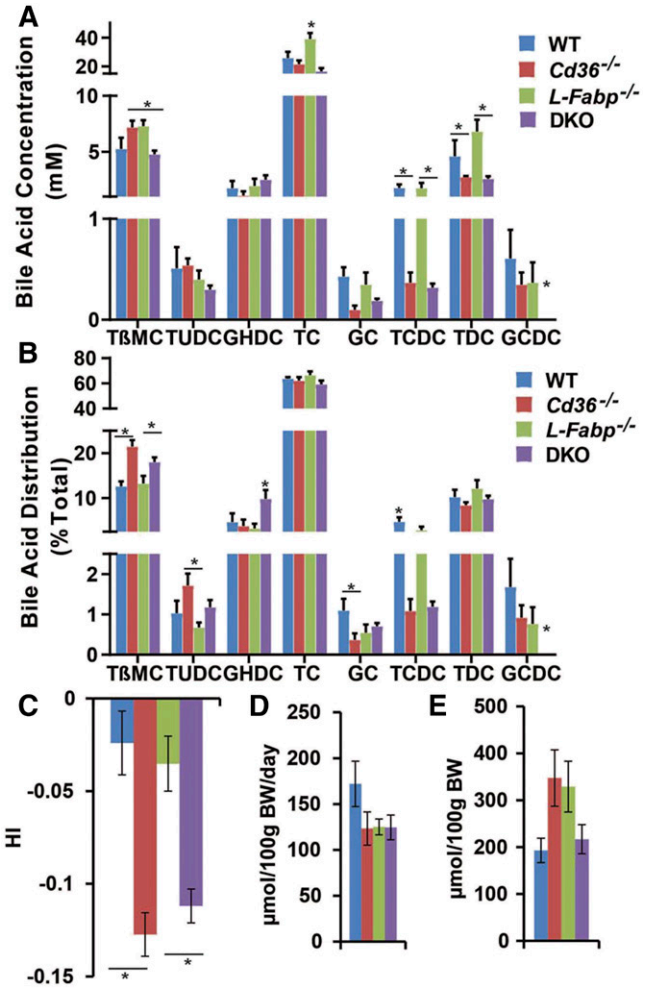

Fig. 2. Bile acid species, hydrophobicity, fecal bile acid excretion, and pool size in LD-fed mice. A, B: Biliary bile was collected from mice fed a LD for 2 weeks, and bile acid species were determined by HPLC as described in Materials and Methods. A: Biliary bile acid concentrations revealed an increase in taurocholate (TC) in L-Fabp$^{-/-}$ mice with a decrease in taurochenodeoxycholate (TCDC) and taurodeoxycholate (TDC) concentration in Cd36$^{-/-}$ and DKO mice compared with WT mice. B: Bile acid species distribution was altered in Cd36$^{-/-}$ and DKO mice, with increased abundance of relatively hydrophilic bile acids tauro-β-muricholate (TβMC), tauroursodeoxycholate (TUDC), and glycohyodeoxycholate (GHDC) (DKO), and decreased abundance of hydrophobic bile acids glycocholate (GC), TCDC, and glycochenodeoxycholate (GCDC). C: Hydrophobicity index (HI) of biliary bile from representative animals of the four genotypes was calculated by using published algorithms (Materials and Methods), revealing a significant reduction in Cd36$^{-/-}$ and DKO mice compared with either WT or L-Fabp$^{-/-}$ mice. D: Fecal bile acid excretion (µmol per 100 g of bw per day) was comparable across the four genotypes. Mice were individually housed, and feces were collected for up to 72 h. Fecal bile acids were extracted and quantitated enzymatically. E: Bile acid pool size (µmol per 100 g of bw) was comparable in four genotypes. Liver, gallbladder, and the entire small and large intestine were pooled and subjected to ethanolic bile acid extraction. Total bile acid mass was measured enzymatically. The data are the mean ± SE (n = 4–8 per group). *Statistically significant differences ($P < 0.05$).

any of the physical parameters of score or gallbladder volume and no differences by genotype in hepatic lipid or bile acid content (Fig. 5D–H). These findings, coupled with the data alluded to above, suggest that neither intestine-specific nor hepatocyte-specific *Cd36* deletion alone can replicate the protection against LD-induced gallstones observed in germline *Cd36*$^{-/-}$ mice.

Increased gallbladder contractility and reduced lipid accumulation in *Cd36*$^{-/-}$ mice

We observed over the course of these studies that the gallbladders of *Cd36*$^{-/-}$ mice appeared smaller and more contracted than their WT controls (**Fig. 6A**). This observation prompted us to examine in more detail a possible role for CD36 in gallbladder function. We confirmed that CD36 expression was undetectable in gallbladder mRNA from *Cd36*$^{-/-}$ mice (Fig. 6B) and that gallbladder CD36 mRNA abundance was indistinguishable between WT (C57BL6/J), *Cd36* flox controls, *Cd36-IKO*, and *Cd36-LKO* mice, suggesting that neither intestine-specific (i.e., villin) nor liver-specific (i.e., albumin) Cre drivers are active in gallbladder mucosa (Fig. 6C). Because prior work has shown a dominant role for gallbladder hypomotility in increased gallstone susceptibility (19, 32), either via decreased CCK production or decreased CCK receptor expression (18), we examined gallbladder contractility using in vitro preparations of gallbladders from WT and *Cd36*$^{-/-}$ mice (Materials and Methods). We observed that gallbladder contractility was increased in response to increasing doses of KCl and methacholine in *Cd36*$^{-/-}$ mice (Fig. 6D, E) and that both the maximum force of contraction and the rate of smooth muscle contraction were increased in *Cd36*$^{-/-}$ mice (Fig. 6F). These findings provide direct functional support for the suggestion that increased gallbladder contractility in *Cd36*$^{-/-}$ and DKO mice might contribute to the protection observed against gallstone formation. We also examined parameters of inflammation in the gallbladders of LD-fed mice because prior work has suggested altered inflammasome induction in response to cholesterol-modulated pathways in atherosclerosis (33). These findings demonstrated an inconsistent adaptive pattern of mRNAs encoding proinflammatory and antiinflammatory mediators (Fig. 6G), with decreased expression of TNFa, but increased expression of TLR2, TLR4, IL1b, IL18, and Nlrp3 in *Cd36*$^{-/-}$ mice. Histologic examination of gallbladders from LD-fed WT and *Cd36*$^{-/-}$ mice (Fig. 6H) revealed mucosal hypertrophy and increased submucosal thickening only in WT mice, with no obvious inflammatory changes evident in gallbladders from *Cd36*$^{-/-}$ mice. Finally, we asked whether the changes observed above in gallbladder function were associated with alterations in lipid accumulation. These findings revealed a trend to reduced accumulation of all lipid classes analyzed, with reduced free cholesterol reaching statistical significance (Fig. 6I). Taken together, the findings indicate that a range of adaptive changes in gallbladder mucosal function and lipid accumulation likely contribute to the protection against gallstone formation.

DISCUSSION

The central findings of these studies are that *Cd36*$^{-/-}$ mice are protected against LD-induced gallstones, through

TABLE 2. Biliary lipid secretion in LD-fed mice of the indicated genotype

Genotype	TC	PL	BA	Flow rate
WT (12)	210.5 ± 6.9[a]	646.7 ± 14.9[a]	5103.8 ± 233.7[a]	91.6 ± 1.2
Cd36$^{-/-}$ (7)	175.1 ± 8.6[a]	603.3 ± 24.1[a]	4827.9 ± 302.6[a]	89.3 ± 1.7
L-Fabp$^{-/-}$ (9)	298.3 ± 11.9[b]	985.6 ± 39.9[b]	6907.5 ± 426.3[b]	115.9 ± 4.5
DKO (4)	221.8 ± 8.8[ab]	819.7 ± 31.9[a]	3900.1 ± 589.3[a]	83.2 ± 0.7

Mice from four experimental groups (n per group) were fed a LD for 2 weeks. Bile samples were collected after surgical laparotomy for 1 h. Biliary cholesterol (TC), phospholipids (PLs), and bile acids (BAs) were analyzed (Materials and Methods). Biliary lipid secretion is expressed as nmol/min/kg bw. Flow rate is expressed as μl/min/kg bw. The difference between values associated with different superscript letters for the parameters indicated in each vertical column is statistically significant ($P < 0.05$).

adaptive mechanisms that include alterations in biliary cholesterol secretion and bile acid composition, as well as increased gallbladder contractility. In addition, *Cd36*$^{-/-}$ mice crossed into *L-Fabp*$^{-/-}$ mice were also protected, reversing the gallstone susceptibility phenotype previously observed in *L-Fabp*$^{-/-}$ mice (12). However, and despite evidence demonstrating adaptive alterations in cholesterol and bile acid metabolic pathways in both the intestine and liver of germline *Cd36*$^{-/-}$ mice, we found that neither intestine-specific nor liver-specific *Cd36* deletion alone was capable of replicating the protection phenotype. Several aspects of these conclusions merit additional consideration.

Our initial hypothesis that *Cd36*$^{-/-}$ mice might be protected against LD-induced gallstones was based on findings that these mice exhibit decreased intestinal cholesterol absorption and trafficking (15, 16). We reasoned that decreased cholesterol absorption in *Cd36*$^{-/-}$ mice might prevent gallstone formation in a manner analogous to ezetimibe treatment (34, 35). However, it seemed equally plausible that *Cd36*$^{-/-}$ mice might actually exhibit increased susceptibility to LD-induced gallstone formation, based on other work showing that genetic strategies that mitigate high-fat diet-induced hepatic steatosis in mice (such as deletion of *Elovl6* or of *L-Fabp*) demonstrated accelerated gallstone formation (12, 13). The current findings point to a gallstone-protection phenotype in LD-fed *Cd36*$^{-/-}$ mice with changes in both intestinal and hepatic pathways contributing to complementary adaptations in cholesterol and bile acid metabolism, but with no dominant protective mechanism.

Having demonstrated that germline *Cd36*$^{-/-}$ mice were protected against LD-induced gallstone formation, we were initially surprised that intestine-specific *Cd36* deletion failed to replicate a protection phenotype. As noted above, this hypothesis was predicated in part on prior findings that intestinal cholesterol absorption is decreased in *Cd36*$^{-/-}$ mice (15, 16). However, we recalled that the alterations observed in intestinal cholesterol uptake and processing in chow-fed *Cd36*$^{-/-}$ mice are regionally specific (proximal greater than distal), and it remains to be determined whether net cholesterol absorption and flux from the intestine is altered in *Cd36*$^{-/-}$ mice fed a cholic acid-supplemented LD. By way of comparison, we previously observed decreased intestinal cholesterol absorption in chow-fed *L-Fabp*$^{-/-}$ mice (12), yet we found no differences (from WT controls) in cholesterol absorption when those mice were fed the LD. These observations diminish the likelihood that genetically manipulated mice might be protected against gallstone formation simply by virtue of decreased intestinal cholesterol absorption.

We considered an alternative hypothesis to account for the protection against gallstones in *Cd36*$^{-/-}$ mice, namely, that compensatory adaptations in hepatic metabolic pathways might mitigate the impact of LD-induced abnormalities. In considering this hypothesis, we were guided by prior findings demonstrating that hepatic CD36 expression increases upon high-fat feeding (as in our LD model; Fig. 5C) (14) and also findings in a line of liver-specific *Cd36* KO mice demonstrating protection against high-fat diet-induced hepatic steatosis, along with decreased hepatic fatty acid uptake (36). Other findings, however, have challenged the conclusions that hepatic fatty acid uptake is decreased in *Cd36*$^{-/-}$ mice (31, 37). In particular, those studies pointed to a role for CD36 in regulating both de novo lipogenesis and also VLDL secretion as key considerations (31, 37). The observation that hyperphagic *ob/ob* mice crossed into *Cd36*$^{-/-}$ mice manifested increased hepatic steatosis because of decreased VLDL secretion (37) might have special relevance to this discussion. This proposed function of CD36 in regulating hepatic VLDL secretion reminded us of our previous findings that liver-specific *Mttp* deletion (*Mttp-LKO* mice) reduced LD-induced gallstone formation because we showed that crossing *Mttp-LKO* mice into *L-Fabp*$^{-/-}$ mice conferred protection against LD-induced gallstones (38). Accordingly, those findings in *ob/ob* mice crossed into *Cd36*$^{-/-}$ mice (37) reinforced the possibility that a hepatocyte-specific pathway of altered lipid metabolism (either altered de novo lipogenesis and/or decreased VLDL secretion) might attenuate gallstone susceptibility in *Cd36-LKO* mice. However, because this was not the case, we conclude that hepatocyte-specific functions of CD36 cannot alone account for the gallstone protection phenotype observed in *Cd36*$^{-/-}$ mice. We cannot definitively explain the observation that CD36 mRNA expression in whole liver extracts appeared to increase after LD feeding (Fig. 5C), although we recognize that other, nonhepatocyte populations (macrophages and Kupffer cells) express CD36 (17), and it is plausible that LD feeding induces adaptive increases in CD36 expression in these cell types. However, this possibility remains to be tested experimentally.

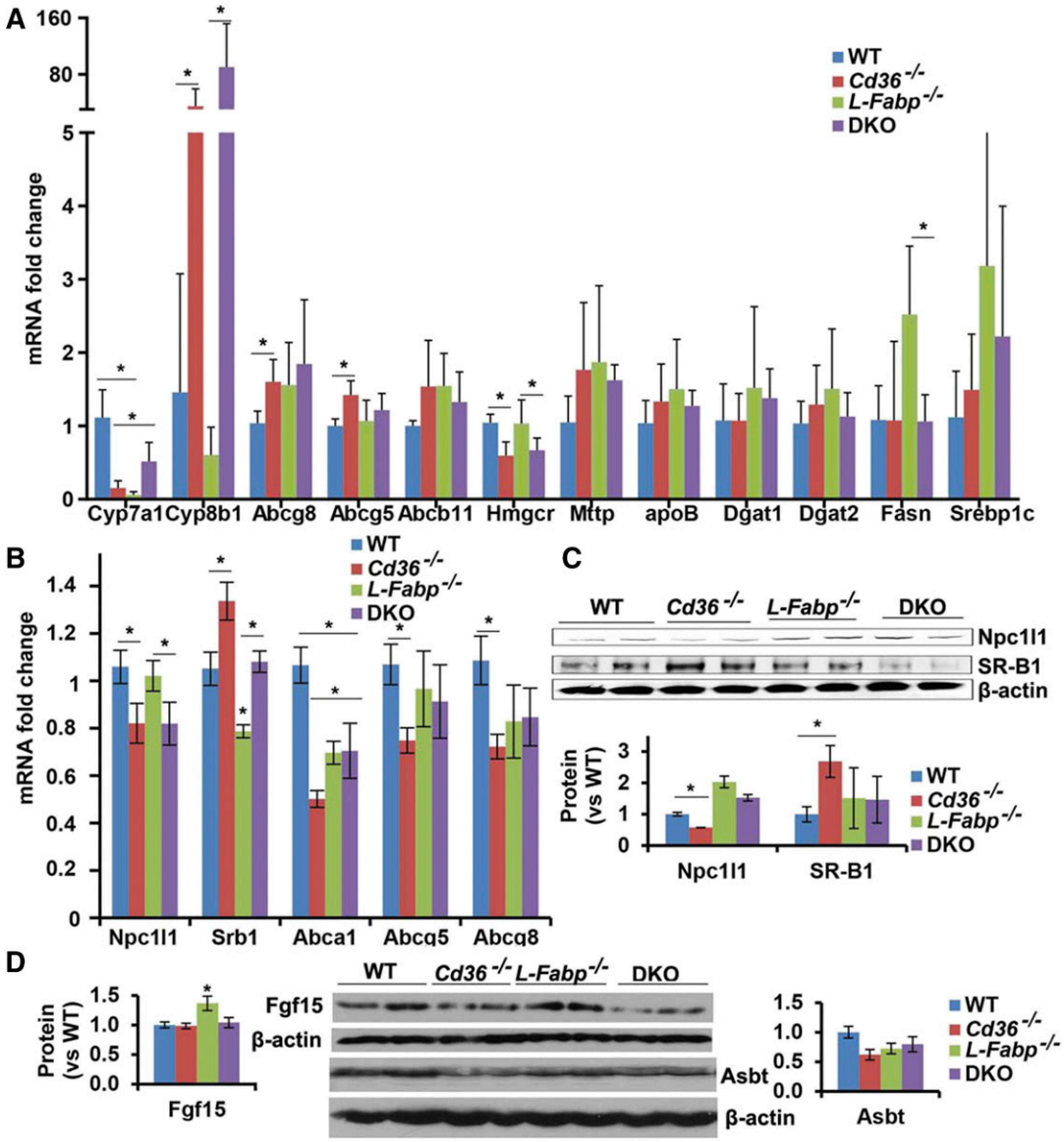

Fig. 3. Adaptive changes in hepatic and intestinal gene expression in LD-fed mice of the indicated genotypes. A, B: RNA was extracted from liver or scraped proximal intestinal mucosa, and mRNA abundance was determined by Real-time quantitative PCR. A: Hepatic mRNA expression. B: Proximal intestinal mRNA expression. C: NPC1L1 and SR-B1 protein expression in proximal intestinal mucosa. Thirty micrograms of protein was separated by SDS-PAGE gel, and the indicated proteins were detected by Western blot (upper). Band density was quantitated, and the data are presented as the mean ± SE (lower). D: Protein was extracted from terminal ileum and aliquots of total homogenate (Fgf15) or purified apical membranes (Asbt) separated on SDS-PAGE gel, and the indicated protein was detected by Western blot. The relative abundance of Fgf15 and Asbt were quantitated by using a Kodak image system, and the data are presented as the mean ± SE. *Statistically significant differences ($P < 0.05$).

As a final consideration, we examined the possibility that altered smooth muscle function and, in particular, altered gallbladder motility might play a role in the protection observed. Our observations point to yet another function for CD36, specifically in regulating gallbladder contractility. Several studies have demonstrated that reduced gallbladder and small intestinal motility promotes gallstone formation (19, 32, 34). Our current observations of increased gallbladder contractility along with the visual appearance of smaller gallbladders in *Cd36*$^{-/-}$ mice might appear somewhat unexpected, based on prior work demonstrating reduced enteroendocrine cell production of CCK and secretin in *Cd36*$^{-/-}$ mice (20). Nevertheless, it is important to note that these contractility studies were conducted in vitro, and we did not independently validate changes in circulating CCK or secretin levels in *Cd36*$^{-/-}$ mice fed a LD. In addition, although those prior studies demonstrated no change in gastric emptying in chow-fed *Cd36*$^{-/-}$ mice (20), we did not independently examine intestinal transit or motility in LD-fed mice, as reported by others (34). Accordingly, conclusions regarding alterations in intestinal motility and other details of gallbladder function that may be regulated by CD36 remain to be examined. However, we would predict that, because gallbladder CD36

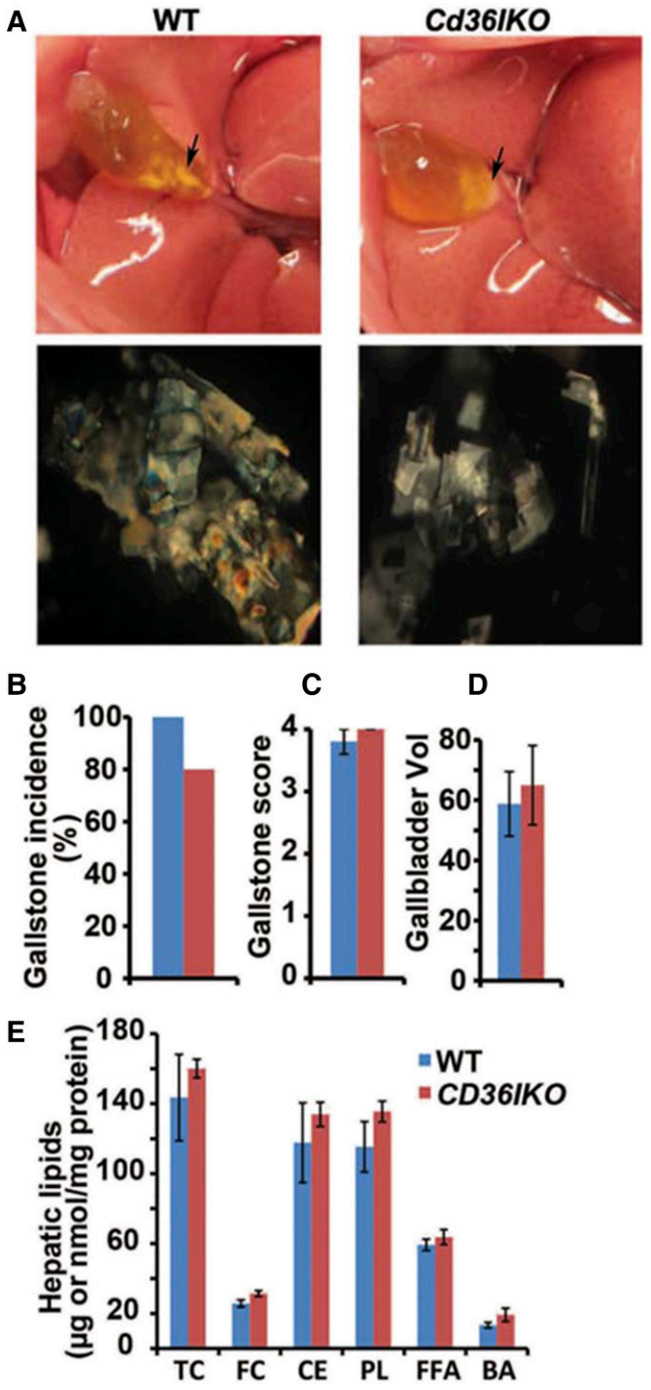

Fig. 4. Intestine-specific Cd36 deletion does not protect against LD-induced gallstone formation. Cd36-IKO mice and their littermate flox/flox controls were fed a LD for 4 weeks. A: Visible gallstones were observed in both genotypes (upper). Polarizing microscopy revealed aggregated ChMCs in both genotypes (lower; 200×). Gallstone incidence (B), gallstone score (C) and gallbladder volume (D) was determined as described in Materials and Methods. E: Hepatic lipids were extracted and quantitated enzymatically (Materials and Methods). Hepatic lipid content is expressed as µg/mg protein, except FFA, which is expressed as nmol/mg protein. The data in C–E represent the mean ± SE. n = 4–6 per group. BA, bile acid, CE, cholesteryl ester; FC, free cholesterol; PL, phospholipid; TC, total cholesterol.

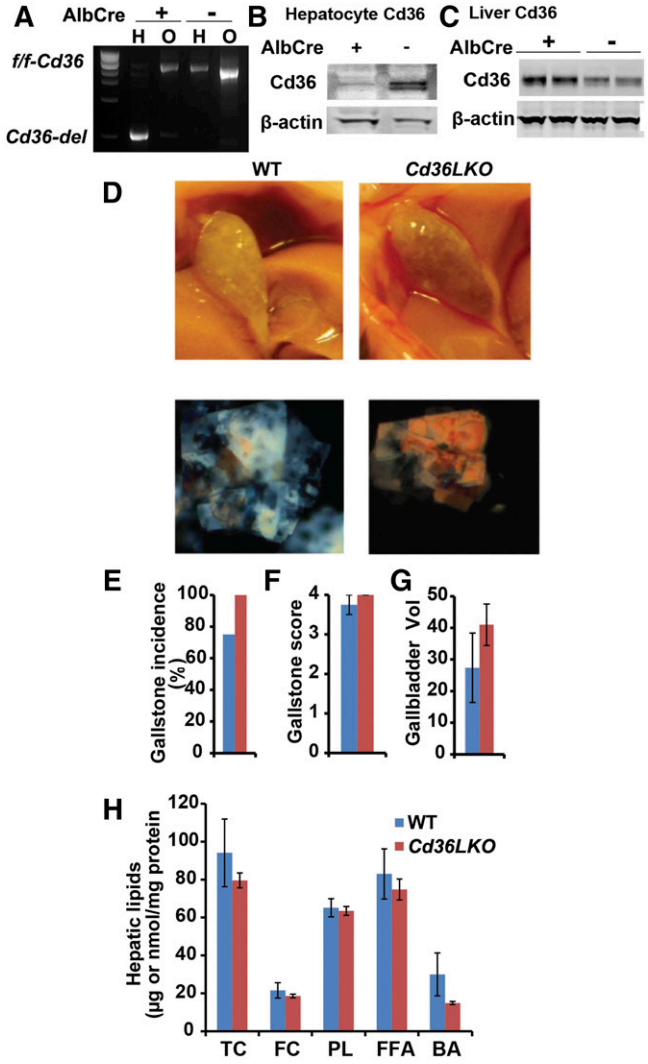

Fig. 5. Hepatocyte-specific Cd36 deletion does not protect against LD-induced gallstone formation. Cd36-LKO mice were generated as described (Materials and Methods). A: DNA was extracted from hepatocytes (H) and the remnant, nonhepatocyte fraction of cells (O) after liver perfusion, and the DNA was analyzed by agarose gel. The hepatocyte fraction from Cd36- LKO mice shows Cre-mediated recombination. B: Hepatocytes were prepared from chow-fed Cd36-LKO mice and flox/flox controls, and extracts were subjected to Western blotting for CD36. C: Whole liver extracts were prepared from Cd36-LKO mice and flox/flox controls fed LD for 4 weeks and Western-blotted for CD36. D: Visible gallstones were observed in both Cd36-LKO and littermate control gallbladders (representative gross appearances of gallbladder in upper). Polarizing microscopy revealed aggregated ChMCs in both genotypes (lower; 200×). Gallstone incidence (E), gallstone score (F), and gallbladder volume (G) were determined as described in Materials and Methods. H: Hepatic lipids were extracted and quantitated enzymatically (Materials and Methods). Hepatic lipid content is expressed as µg/mg protein except FFA, which is expressed as nmol/mg protein. The data in C–E represent the mean ± SE. n = 4–6 per group. BA, bile acid, FC, free cholesterol; PL, phospholipid; TC, total cholesterol.

mRNA was unaltered in either *Cd36-IKO* or *Cd36-LKO* mice (Fig. 6C), it would be unlikely that a cross between the liver- and intestine-specific *Cd36* KO lines would yield a gallstone protection phenotype. This prediction has yet to be tested, but at least raises, in principle, the possibility (alluded to above) that alterations in yet other, cell-specific CD36-dependent pathways might be relevant to gallstone pathogenesis.

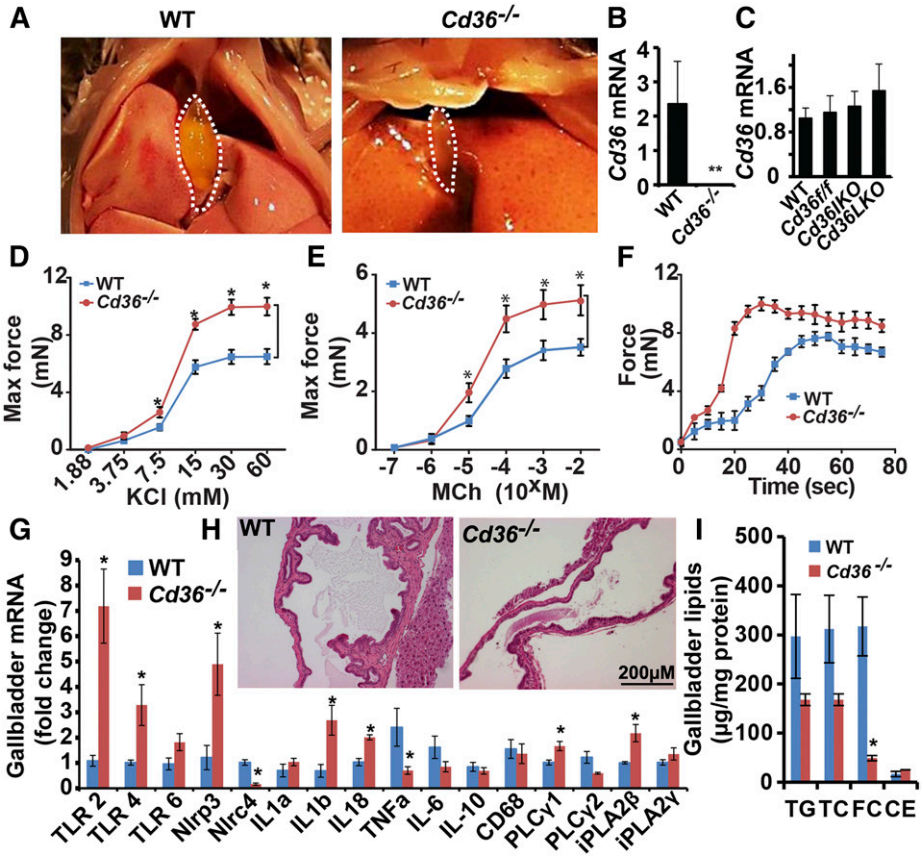

Fig. 6. Gallbladder contractility is increased in Cd36$^{-/-}$ mice. A: Mice of the indicated genotype were euthanized after a 4 h fast, and the gallbladder was visualized after laparotomy performed under anesthesia. B: Cd36 mRNA expression in gallbladder showed loss of Cd36 expression in Cd36$^{-/-}$mice. C: No change in Cd36 mRNA expression comparing WT, Cd36 flox, Cd36-IKO, and Cd36-LKO gallbladder. D, E: Gallbladder contractility was studied in vitro in response to the indicated agonists. Increased contractility was found in gallbladders from Cd36$^{-/-}$ mice in response to both potassium chloride (D) and methacholine (E), compared with congenic WT controls. F: The contractile force of gallbladders of the indicated genotype is shown. G: RNA was extracted from gallbladders of the indicated genotype of LD-fed mice, and mRNA expression of candidate genes was determined by qPCR. The data are the mean ± SE. *Statistically significant differences ($P < 0.05$). H: Morphological appearance of gallbladders from LD-fed mice of the indicated genotype (hematoxylin and eosin stain; magnification ×200). I: Gallbladder lipids were extracted and quantitated enzymatically (Materials and Methods). Gallbladder lipid content is expressed as μg/mg protein. The data in B–G and I represent the mean ± SE, n = 3–6 per group. CE, cholesteryl ester; FC, free cholesterol; TC, total cholesterol; TG, triglyceride.

REFERENCES

1. Peery, A. F., E. S. Dellon, J. Lund, S. D. Crockett, C. E. McGowan, W. J. Bulsiewicz, L. M. Gangarosa, M. T. Thiny, K. Stizenberg, D. R. Morgan, et al. 2012. Burden of gastrointestinal disease in the United States: 2012 update. *Gastroenterology.* **143:** 1179–1187.e1–3.
2. Di Ciaula, A., D. Q. Wang, G. Garruti, H. H. Wang, I. Grattagliano, O. de Bari, and P. Portincasa. 2014. Therapeutic reflections in cholesterol homeostasis and gallstone disease: a review. *Curr. Med. Chem.* **21:** 1435–1447.
3. Lammert, F., and T. Sauerbruch. 2005. Mechanisms of disease: the genetic epidemiology of gallbladder stones. *Nat. Clin. Pract. Gastroenterol Hepatol.* **2:** 423–433.
4. Joshi, A. D., C. Andersson, S. Buch, S. Stender, R. Noordam, L. C. Weng, P. E. Weeke, P. L. Auer, B. Boehm, C. Chen, et al. 2016. Four susceptibility loci for gallstone disease identified in a meta-analysis of genome-wide association studies. *Gastroenterology.* **151:** 351–363.e28.
5. Wang, H. H., X. Li, S. B. Patel, and D. Q. Wang. 2016. Evidence that the adenosine triphosphate-binding cassette G5/G8-independent pathway plays a determinant role in cholesterol gallstone formation in mice. *Hepatology.* **64:** 853–864.
6. Lyons, M. A., and H. Wittenburg. 2006. Cholesterol gallstone susceptibility loci: a mouse map, candidate gene evaluation, and guide to human LITH genes. *Gastroenterology.* **131:** 1943–1970.
7. Lyons, M. A., H. Wittenburg, R. Li, K. A. Walsh, G. A. Churchill, M. C. Carey, and B. Paigen. 2003. Quantitative trait loci that determine lipoprotein cholesterol levels in DBA/2J and CAST/Ei inbred mice. *J. Lipid Res.* **44:** 953–967.
8. Moschetta, A., A. L. Bookout, and D. J. Mangelsdorf. 2004. Prevention of cholesterol gallstone disease by FXR agonists in a mouse model. *Nat. Med.* **10:** 1352–1358.
9. Cheng, S., M. Zou, Q. Liu, J. Kuang, J. Shen, S. Pu, L. Chen, H. Li, T. Wu, R. Li, et al. 2017. Activation of constitutive androstane receptor prevents cholesterol gallstone formation. *Am. J. Pathol.* **187:** 808–818.
10. Newberry, E. P., Y. Xie, S. M. Kennedy, J. Luo, and N. O. Davidson. 2006. Protection against Western diet-induced obesity and hepatic steatosis in liver fatty acid-binding protein knockout mice. *Hepatology.* **44:** 1191–1205.
11. Newberry, E. P., S. Kennedy, Y. Xie, J. Luo, H. Jiang, D. S. Ory, and N. O. Davidson. 2015. Phenotypic divergence in two lines of L-Fabp−/− mice reflects substrain differences and environmental modifiers. *Am. J. Physiol. Gastrointest. Liver Physiol.* **309:** G648–G661.
12. Xie, Y., E. P. Newberry, S. M. Kennedy, J. Luo, and N. O. Davidson. 2009. Increased susceptibility to diet-induced gallstones in liver fatty acid binding protein knockout mice. *J. Lipid Res.* **50:** 977–987.
13. Kuba, M., T. Matsuzaka, R. Matsumori, R. Saito, N. Kaga, H. Taka, K. Ikehata, N. Okada, T. Kikuchi, H. Ohno, et al. 2015. Absence of

Elovl6 attenuates steatohepatitis but promotes gallstone formation in a lithogenic diet-fed Ldlr(−/−) mouse model. *Sci. Rep.* **5:** 17604.
14. Koonen, D. P., R. L. Jacobs, M. Febbraio, M. E. Young, C. L. Soltys, H. Ong, D. E. Vance, and J. R. Dyck. 2007. Increased hepatic CD36 expression contributes to dyslipidemia associated with diet-induced obesity. *Diabetes.* **56:** 2863–2871.
15. Nauli, A. M., F. Nassir, S. Zheng, Q. Yang, C. M. Lo, S. B. Vonlehmden, D. Lee, R. J. Jandacek, N. A. Abumrad, and P. Tso. 2006. CD36 is important for chylomicron formation and secretion and may mediate cholesterol uptake in the proximal intestine. *Gastroenterology.* **131:** 1197–1207.
16. Nassir, F., B. Wilson, X. Han, R. W. Gross, and N. A. Abumrad. 2007. CD36 is important for fatty acid and cholesterol uptake by the proximal but not distal intestine. *J. Biol. Chem.* **282:** 19493–19501.
17. Yu, M., M. Jiang, Y. Chen, S. Zhang, W. Zhang, X. Yang, X. Li, Y. Li, S. Duan, J. Han, et al. 2016. Inhibition of macrophage CD36 expression and cellular oxidized low density lipoprotein (oxLDL) accumulation by tamoxifen: a peroxisome proliferator-activated receptor (PPAR)gamma-dependent mechanism. *J. Biol. Chem.* **291:** 16977–16989.
18. Wang, D. Q., F. Schmitz, A. S. Kopin, and M. C. Carey. 2004. Targeted disruption of the murine cholecystokinin-1 receptor promotes intestinal cholesterol absorption and susceptibility to cholesterol cholelithiasis. *J. Clin. Invest.* **114:** 521–528.
19. Wang, H. H., M. Liu, P. Portincasa, P. Tso, and D. Q. Wang. 2016. Lack of endogenous cholecystokinin promotes cholelithogenesis in mice. *Neurogastroenterol. Motil.* **28:** 364–375.
20. Sundaresan, S., R. Shahid, T. E. Riehl, R. Chandra, F. Nassir, W. F. Stenson, R. A. Liddle, and N. A. Abumrad. 2013. CD36-dependent signaling mediates fatty acid-induced gut release of secretin and cholecystokinin. *FASEB J.* **27:** 1191–1202.
21. Febbraio, M., N. A. Abumrad, D. P. Hajjar, K. Sharma, W. Cheng, S. F. Pearce, and R. L. Silverstein. 1999. A null mutation in murine CD36 reveals an important role in fatty acid and lipoprotein metabolism. *J. Biol. Chem.* **274:** 19055–19062.
22. Cifarelli, V., S. Ivanov, Y. Xie, N. H. Son, B. T. Saunders, T. A. Pietka, T. M. Shew, J. Yoshino, S. Sundaresan, N. O. Davidson, et al. 2017. CD36 deficiency impairs the small intestinal barrier and induces subclinical inflammation in mice. *Cell. Mol. Gastroenterol. Hepatol.* **3:** 82–98.
23. Carey, M. C. 1978. Critical tables for calculating the cholesterol saturation of native bile. *J. Lipid Res.* **19:** 945–955.
24. Heuman, D. M. 1989. Quantitative estimation of the hydrophilic-hydrophobic balance of mixed bile salt solutions. *J. Lipid Res.* **30:** 719–730.
25. Dawson, P. A., M. Hubbert, J. Haywood, A. L. Craddock, N. Zerangue, W. V. Christian, and N. Ballatori. 2005. The heteromeric organic solute transporter alpha-beta, Ostalpha-Ostbeta, is an ileal basolateral bile acid transporter. *J. Biol. Chem.* **280:** 6960–6968.
26. Newberry, E. P., Y. Xie, S. Kennedy, X. Han, K. K. Buhman, J. Luo, R. W. Gross, and N. O. Davidson. 2003. Decreased hepatic triglyceride accumulation and altered fatty acid uptake in mice with deletion of the liver fatty acid-binding protein gene. *J. Biol. Chem.* **278:** 51664–51672.
27. Tharp, K. M., A. Khalifeh-Soltani, H. M. Park, D. A. Yurek, A. Falcon, L. Wong, R. Feng, K. Atabai, and A. Stahl. 2016. Prevention of gallbladder hypomotility via FATP2 inhibition protects from lithogenic diet-induced cholelithiasis. *Am. J. Physiol. Gastrointest. Liver Physiol.* **310:** G855–G864.
28. Kudo, M., S. M. Khalifeh Soltani, S. A. Sakuma, W. McKleroy, T. H. Lee, P. G. Woodruff, J. W. Lee, K. Huang, C. Chen, M. Arjomandi, et al. 2013. Mfge8 suppresses airway hyperresponsiveness in asthma by regulating smooth muscle contraction. *Proc. Natl. Acad. Sci. USA.* **110:** 660–665.
29. Chiang, J. Y. 2009. Bile acids: regulation of synthesis. *J. Lipid Res.* **50:** 1955–1966.
30. Kim, I., S. H. Ahn, T. Inagaki, M. Choi, S. Ito, G. L. Guo, S. A. Kliewer, and F. J. Gonzalez. 2007. Differential regulation of bile acid homeostasis by the farnesoid X receptor in liver and intestine. *J. Lipid Res.* **48:** 2664–2672.
31. Clugston, R. D., J. J. Yuen, Y. Hu, N. A. Abumrad, P. D. Berk, I. J. Goldberg, W. S. Blaner, and L. S. Huang. 2014. CD36-deficient mice are resistant to alcohol- and high-carbohydrate-induced hepatic steatosis. *J. Lipid Res.* **55:** 239–246.
32. Wang, H. H., P. Portincasa, M. Liu, P. Tso, L. C. Samuelson, and D. Q. Wang. 2010. Effect of gallbladder hypomotility on cholesterol crystallization and growth in CCK-deficient mice. *Biochim. Biophys. Acta.* **1801:** 138–146.
33. Sheedy, F. J., A. Grebe, K. J. Rayner, P. Kalantari, B. Ramkhelawon, S. B. Carpenter, C. E. Becker, H. N. Ediriweera, A. E. Mullick, D. T. Golenbock, et al. 2013. CD36 coordinates NLRP3 inflammasome activation by facilitating intracellular nucleation of soluble ligands into particulate ligands in sterile inflammation. *Nat. Immunol.* **14:** 812–820.
34. Xie, M., V. R. Kotecha, J. D. Andrade, J. G. Fox, and M. C. Carey. 2012. Augmented cholesterol absorption and sarcolemmal sterol enrichment slow small intestinal transit in mice, contributing to cholesterol cholelithogenesis. *J. Physiol.* **590:** 1811–1824.
35. Portincasa, P., and D. Q. Wang. 2017. Effect of inhibition of intestinal cholesterol absorption on the prevention of cholesterol gallstone formation. *Med. Chem.* Epub ahead of print. February 9, 2017; doi:10.2174/1573406413666170209122851.
36. Wilson, C. G., J. L. Tran, D. M. Erion, N. B. Vera, M. Febbraio, and E. J. Weiss. 2016. Hepatocyte-specific disruption of CD36 attenuates fatty liver and improves insulin sensitivity in HFD-fed mice. *Endocrinology.* **157:** 570–585.
37. Nassir, F., O. L. Adewole, E. M. Brunt, and N. A. Abumrad. 2013. CD36 deletion reduces VLDL secretion, modulates liver prostaglandins, and exacerbates hepatic steatosis in ob/ob mice. *J. Lipid Res.* **54:** 2988–2997.
38. Xie, Y., H. Y. Fung, E. P. Newberry, S. Kennedy, J. Luo, R. M. Crooke, M. J. Graham, and N. O. Davidson. 2014. Hepatic Mttp deletion reverses gallstone susceptibility in L-Fabp knockout mice. *J. Lipid Res.* **55:** 540–548.